RSC Advances

ROYAL SOCIETY OF CHEMISTRY

www.rsc.org/advances

Subphthalocyanine as Hole Transporting Material for Perovskite Solar Cells.

Georgia Sfyri[a,b], Challuri Vijay Kumar[a]*, Gokulnath Sabapathi[c], Lingamallu Giribabu[c], Konstantinos S. Andrikopoulos[a], Elias Stathatos[d] and Panagiotis Lianos[a,e]*

[a]FORTH/ICE-HT, P.O. Box 1414, 26504 Patras, Greece

[b]Physics Department, University of Patras, 26500 Patras, Greece

[c]Inorganic and Physical Chemistry Division, Indian Institute of Chemical Technology, Hyderabad,500 007, India.

[d]Electrical Engineering Department, Technological–Educational Institute of Western Greece, 26334 Patras, Greece

[e]Department of Chemical Engineering, University of Patras, 26500 Patras, Greece

Key words: perovskite, solar cells, hole transport material, subphthalocyanine.

CORRESPONDING AUTHORS: challuri.iict@gmail.com and lianos@upatras.gr Tel: ++30 2610 997513 Fax: ++30 2610 997803

Abstract

Non planar 14 –π aromatic subphthalocyanine has been introduced for the first time as hole transporting material for organometal halide perovskite solar cells and achieved a power conversion efficiency of 6.6%. Cells stored in the dark under ambient conditions underwent an incubation period of nine days during which, we observed an increase in efficiency followed by slow progressive deterioration. However, Raman spectral analysis of pristine perovskite deposited on titania revealed a much faster degradation thus indicating that the subphthalocyanine layer provides a temporary protection to the underlying perovskite layer.

INTROUDUCTION

Hybrid organic–inorganic solar cells based on organo lead halide perovskites have attracted significant attention over the last three years thanks to their impressive conversion efficiencies and the intriguing intrinsic properties of organo lead halide perovskites.[1-6] Efficient light-absorbing sensitizers and inorganic semiconducting metal oxides must be paired with an efficient organic hole transporting material (HTM) in order to establish appropriate regenerative cycles for the holes left in the oxidized sensitizers after photon absorption and electron injection. Currently, the most popular HTM is the single molecule spiro–OMeTAD, which has offered power conversion efficiencies (PCE) of over 15%, based on various device structures[4,7]. Most recent developments have reached the impressive PCE values of ~20%.[8, 9, 10]

Despite offering the best performance yet achieved in an HTM, spiro-OMeTAD suffers from high synthesis cost, low hole mobility and low conductivity, which limit its potential for massive future applications of perovskite solar cells. Therefore, the development of other efficient and inexpensive molecular HTMs with optimal electronic properties remains an attractive goal. Recently reported single molecule HTMs, such as 3,4-ethylenedioxythiophene[11], pyrene[12], linear π-conjugated[13], butadiene[14], a spiro-OMeTAD derivative[15] and star-shaped HTMs[16] resulted in high conversion efficiencies of 11–16%. p - Type inorganic semiconductors (i.e., CuI, CuSCN, and NiO)[17,18] and polymeric HTMs [19,20] have also been extensively studied.

We have recently reported copper phthalocyanine as hole transporting material for perovskite solar cells and achieved a PCE of 5%[21]. Torres, Nazeeruddin and coworkers also recently published a non-aggregated Zn(II)octa(2,6-diphenylphenoxy) phthalocyanine [22] (TT80), which was used as HTM for solution processed perovskite solar cells with (bis(trifluoromethane) sulfonimide lithium salt (LiTFSI) and tertbutyl pyridine additives and achieved PCE of 6.7%.

Boron subphthalocyanines (SubPc) have excellent thermal stability and are highly attractive as photon absorbing materials in organic solar cells because their absorbance maximum overlaps almost perfectly with the part of the solar irradiation spectrum with the highest intensity at the earth's surface. The symmetrical 14-π electron configuration of SubPc is of paramount importance for its application as active material in photodynamic therapy[23], non linear optics[24], OLEDs[25], and OPVs[26]. In continuation of our research work on HTM alternatives of spiro-OMETAD, we presently report vacuum processed boron

subphthalocyanine as hole transport material for perovskite solar cells. The PCE achieved with this material reached 6.6% and there is ground for further improvement.

EXPERIMENTAL SECTION

Materials

All materials were purchased from Aldrich, unless otherwise specified, and they were used as received. FTO glasses of 8 ohm/square were purchased from Pilkington.

Methyl ammonium iodide Synthesis

Methylammonium iodide was synthesized by the previously reported procedure[27] by reacting 27.8 ml of methylamine (40 wt% in H_2O) and 30 ml of hydroiodic acid (57 wt% in water) at 0°C for 2 hours. Solid residue was obtained in a rotary evaporator by carefully removing the solvents at 40 °C. The yellow crude product methyl ammonium iodide (CH_3NH_3I) was washed with diethyl ether several times, and then finally recrystallized from a mixed solvent of diethyl ether and ethanol. After filtration, the pure solid was collected and dried at 70 °C in a vacuum oven overnight.

Subphthalocyanine Synthesis

Subphthalocyanine was synthesized with a modified procedure based on the report of Zyskowski et al.[28] Phthalonitrile (1.77 g, 13.8mmol) was dissolved with stirring in 1,2-dichlorobenzene (70 mL) under argon atmosphere. To this solution BCl_3 (9.26 mL of 1.0 M solution (9.26mmol) in heptane) was added in a single portion. On gradual heating the heptane was distilled off. When distillation was complete, the reactants were heated at reflux for an additional 1.5 hours. Then the reaction mixture was cooled to room temperature and the solvent was removed by rotary evaporation. The resulting crude product was purified on a short pad of neutral alumina. The obtained golden-brown powder was then dried in the vacuum oven yielding the compound of **Figure 1**: (1.13 g, 57%). ^{1}H (400 MHz, $CDCl_3$): δ = 7.96-7.98 (6H, m), 8.89-8.94 (6H, m); $\lambda_{max}(CHCl_3)$/nm 564.

Fabrication of Perovskite solar cells

FTO-coated glass substrates were cut in pieces of dimensions 1 cm ×3 cm. One third of the conductive layer was removed using zinc powder and hydrochloric acid. Then they were washed with mild detergent, rinsed several times with distilled water and subsequently

with ethanol in an ultrasonic bath, finally dried under air stream. This patterned and cleaned FTO electrode was first treated in $TiCl_4$ by dipping into a solution made of 0.04M $TiCl_4$ in H_2O for 30 minutes, then copiously rinsing and finally calcining at 500˚C. A compact thin layer of TiO_2 was then deposited by aerosol spray pyrolysis using a solution of 0.2 M Diisopropoxytitanium bis(acetylacetonate) in EtOH. After spraying, the samples were heated for 1 hour at 500˚C. Subsequently, a mesoporous TiO_2 layer composed of titania paste made of P25 nanoparticles was spin coated at 4000 rpm for 30 seconds and then heated for 15 minutes at 500 ˚C. Finally, it was treated again in $TiCl_4$ as above. Active perovskite layer was deposited on the thus prepared titania film by modifying published procedures[27]. A precursor solution was made by mixing 230 mg $PbCl_2$ with 394 mg methyl ammonium iodide in 1 ml of DMF. The atomic ratio Pb:Cl:I in the precursor solution was thus 1:2:3. The solution was kept under stirring for about half an hour and then it was deposited by spin coating at 3000 rpm for 60 seconds under conditions of 15% relative humidity in a dry box. Then it was heated at 80 ˚C for about 45 min, which made the sample's color turn from yellow to black. Hole-transporting SubPc layer was then deposited by vacuum thermal evaporation. The last step was the deposition of 80 nm thick gold electrodes also by thermal evaporation under vacuum. These unit devices had an active size of 15 mm^2 (10 mm x 1.5 mm) as defined by the size of the gold electrodes. A schematic representation of cell components is shown also in **Figure 1**.

Characterization-Methods

Illumination of the samples was made with a PECCELL PEC-L01 Solar Simulator set at 100 mW/cm^2. $J-V$ characteristic curves were recorded under ambient conditions with a Keithley 2601 source meter that was controlled by Keithley computer software (LabTracer). IPCE values were obtained with an Oriel IQE 200 system. UV-vis absorption spectra were recorded using a Shimadzu model 2600 spectrophotometer equipped with an integration sphere. XRD patters were obtained with a D8 Advance Bruker diffractometer and FESEM images with a Zeiss SUPRA 35VP microscope. A T64000 micro Raman system in the triple subtractive configuration was used in order to record Raman spectra down to ~10 cm^{-1}. The excitation wavelength was 514.5 nm while the laser power on the sample was set at particularly low values (10 μW); spectra were also acquired using considerably higher laser power values (0.8 mW). The focusing of the excitation beam was achieved by a 50x microscope objective which offered spatial resolution of ~1 μm. The backscattered photons

were collected at ambient conditions and recorded by a 2D-CCD detector with a spectral resolution of ~2.5 cm^{1}.

RESULTS AND DISCUSSION

Materials characterization

The Pb:Cl:I ratio of the presently synthesized $CH_3NH_3PbCl_xI_{3-x}$ perovskites has been determined by EDX and reported in a previous publication[29] and was 1:1.1:2.2. It indicates that the quantity of iodine is twice as large as that of chlorine. **Figure 2** shows the UV-vis absorption spectra of SubPc on TiO_2 films with and without perovskite. $CH_3NH_3PbCl_xI_{3-x}$ was deposited onto the mesoporus TiO_2 surface by spin coating. After thermal annealing SubPc was deposited by vacuum deposition on the surface of the perovskite. Alternatively, SubPc was vacuum deposited directly on titania. **Figure 2** also shows absorption spectrum of $CH_3NH_3PbCl_xI_{3-x}/TiO_2$ alone. The perovskite nanocrystals absorbed light over the whole visible range. Subphthalocyanine absorbed light in wavelengths between 450-620 nm. When the two materials came together, SubPc contribution markedly distinguished itself, indicating a substantial contribution of SubPc to photon harvesting. Furthermore, **Figure 2** shows the absorption spectrum of the previously studied copper phthalocyanine (CuPc)[21], for comparison. The latter absorbs light in a broader range of the visible spectrum and it has a smaller band gap, i.e. 1.7 eV *vs* 2.0 eV of SubPc. **Figure 3** shows energy levels diagram of the respective components in the solar cell device in comparison with the previously studied CuPc. The HOMO and LUMO levels for SubPc are reported in literature to be -5.6 and -3.6, respectively[30]. These levels may match the corresponding levels of $CH_3NH_3PbCl_xI_{3-x}$ and titania, but they are surely less favorable than those of CuPc. Nevertheless, the cross-sectional FESEM image of **Figure 4** reveals the formation of well-defined layer structure with sharp interfaces. Therefore, the chosen components guarantee successful solar cell assembly.

XRD diffractograms of successive organic layers on titania are presented in **Figure 5**. Perovskite material gave a well-defined XRD pattern but no contribution was detected for SubPc. It is possible that the deposited SubPc film is amorphous or too thin to give a detectable XRD signal.

Solar cell performance

The current voltage *(J-V)* characteristics of the SubPc/$CH_3NH_3PbCl_xI_{3-x}$ /TiO_2-based solar cell, measured under ambient conditions using simulated solar radiation are shown in

Figure 6. Corresponding photovoltaic parameters are shown in **Table 1** in comparison with the previously published[21] CuPc. On the cell assembly day, SubPc cell demonstrated a short circuit current density (J_{sc}) of 14.0 mA/cm^2, an open circuit voltage (*Voc*) of 0.60 V and fill factor (FF) of 40% leading to a PCE 3.4%. However, when the cell was stored under ambient conditions in the dark, it underwent an incubation period of 9 days during which, the efficiency increased. Thus the final measured values were J_{sc}=21.3 mA/cm^2, *Voc*=0.67 V and fill factor of 46% leading to a PCE 6.6%. After the 9th day the cell slowly deteriorated. The corresponding CuPc cells gave J_{sc}=19.2 mA/cm^2, *Voc*=0.67 V and fill factor of 40% leading to a PCE 5.0%. *Voc* of the SubPc and CuPc were the same so the enhancement of power conversion efficiency was mainly due to the improvement of the values of Jsc and FF.

The action spectrum (IPCE%) of the SubPc/$CH_3NH_3PbCl_xI_{3-x}$ /TiO_2 based solar cell is shown in **Figure 2** together with the above discussed absorption spectra. Despite the important contribution of SubPc in light harvesting, the action spectrum does not mark any SubPc contribution. Therefore, SubPc role seems to be limited only to act as HTM. Its superiority *vs* CuPc obviously indicates that it is a better hole transporter. This is only an overall conclusion. More work is necessary to determine structural parameters that may be at the origin of the differentiation between these two materials. All the above comparative data, for example, the light absorption range, the value of the bandgap, the placement of the HOMO and LUMO levels are in favor of CuPc. However, SubPc did give a better performance. The only reasonable explanation is that this has to do with the molecular configuration in each case and the packing of the material in the hole-transporting layer. SubPc is a cone shaped molecule and it is for sure less planar than CuPc[21] or ZnPc[22]. The presence of Cl counter ion may additionally prevent aggregation. It is its molecular configuration what most probably makes the difference.

Micro-Raman Analysis of cell stability

The Raman spectra of $PbCl_2$ and CH_3NH_3I precursors are given in **Figure 7**. Both spectra were collected under inert atmosphere. The Raman spectrum of the $CH_3NH_3PbCl_xI_{3-x}$ perovskite at ambient conditions is also given in the same figure for comparison. It was collected using 0.8 mW laser power, which is a considerably high value for photosensitive materials. The peaks at 515, 397 and 144 cm^{-1} are attributed to TiO_2 (anatase) substrate and the fact that they appear in the spectrum suggests that the laser power is adequate for the photons to reach the substrate and the inelastically scattered light subsequently to reach the

sample's surface and be collected by the objective. The remaining peaks i.e. the ones at 97, 110, 163 and 215 cm^{-1} are attributed to the perovskite layer and more particularly to Pb-I and Pb-Cl bonds in accordance with Ref.[31]. Due to the photosensitivity of the material, structural modifications are expected when the material is illuminated by this value of laser power and for this reason it has been reported[31] that laser power in the order of 10 μW should be used in order to minimise photodegradation effects. The stability of the sample over time was checked by the collection of a series of spectra at regular intervals using low laser power (10 μW) on the sample (**Figure 8**). Despite the low signal to noise ratio, three peaks assigned to the perovskite layer can be clearly resolved together with a weak anatase mode at ~145 cm^{-1}. Using the intensity of the latter peak as a reference, the intensity of the perovskite bands may be weighted as a function of time. **Figure 8b** depicts the intensity ratios of two of the perovskite bands ~96 cm^{-1} and ~109 cm^{-1} with respect to the reference anatase band (~145 cm^{-1}) as a function of time up to approximately 2 days. The intensity of both bands decreased with time, indicating degradation of the material at ambient conditions. More specifically, the intensity of the 96 cm^{-1} band decreased slightly faster than the respective intensity of the 109 cm^{-1} band. The latter is not easily explained, however, it may be attributed to the different stabilities of the Pb polyhedral species containing different amounts of Cl and I.

The data of the previous sub-section showed that the fully assembled cells underwent an incubation period of 9 days and after that period the degradation could be detected. The Raman spectra analysis showed that pristine perovskite rapidly degraded in a period of two days. Vulnerability of organo-lead halide perovskites is mainly due to moisture[31-33]. It is then concluded that the placement of SubPc on the top slows down the degradation process.

CONCLUSIONS

We have introduced a thermally evaporated, boron subphthalocyanine as hole transporting material for organo lead halide perovskite solar cells. The devices were optimized and gave satisfactory performance of power conversion efficiency 6.6%. These results show the potential of sub phthalocyanine as hole transporting material for cost effective solid state lead halide perovskite solar cells. Raman spectral analysis of titania-deposited pristine $CH_3NH_3PbCl_xI_{3-x}$ layer indicated fast degradation under ambient conditions. However, when the perovskite was covered with SubPc this degradation was slowed down, indicating the importance of the necessity for protective measures to preserve organometal halide perovskites from degradation.

ACKNOWLEDGEMENTS

The present work was supported by the project 11SYN_7_298, implemented under the Act "COOPERATION 2011 - Partnerships of Production and Research Institutions in Focused Research and Technology" of the Operational Programmes “Competitiveness and Entrepreneurship (EPAN II)” and “Regions in Transmission (NSFR 2007-13)”. The authors are very thankful to Dr.V.Dracopoulos for his help with XRD and FESEM measurements.

REFERENCES

1.A. Kojima, K. Teshima, Y. Shirai, T. Miyasaka, *J. Am. Chem. Soc.,*2009**, 131**, 6050-6051.

2.J.-H. Im, C.-R. Lee, J.-W. Lee, S.-W. Park, and N.-G. Park, *Nanoscale*, 2011**, 3**, 4088-4093.

3.H.-S. Kim, C.-R. Lee, J.-H. Im, K.-B. Lee, T. Moehl, A. Marchioro, A. S.-J. Moon, R. Humphry-Baker, J.-H. Yum, J. E. Moser, M.Grätzel, N.-G. Park, . *Sci. Rep***,** 2012, ***2***,591-597.

4.J. Burschka, N. Pellet, S.-J. Moon, R. Humphry-Baker, P. Gao, M. K. Nazeeruddin, and M. Grätzel, *Nature*, 2013**, 499**, 316-319.

5.M. Z. Liu, M. B. Johnston, and H. J. Snaith, *Nature*, 2013**, 501**, 395-398.

6. J.-H. Heo, S. H. Im, J. H. Noh, T. N. Mandal, C.-S. Lim, J. A. Chang, Y. H. Lee, H.-J. Kim, A. Sarkar, M. K. Nazeeruddin, M. Grätzel, and S. I. Seok, *Nat. Photonics*, 2013**,** 7, 486-491.

7.K. Wojciechowski , M. Saliba , T. Leijtens , A. Abate , H. J. Snaith , *Energy Environ. Sci.* 2014, **7** , 1142-1147 .

8. S. Kazim, M. K. Nazeeruddin, M. Grätzel, S. Ahmad, *Angew. Chem. Int. Ed.* 2014, **53**, 2812–2824; *Angewandte Chemie*, 2014, **126**, 2854– 2867.

9. M. A. Green, A. Ho-Baillie, H. J. Snaith, *Nat. Photon.,* 2014, **8**, 506– 514;

10.V. W. Bergmann, S. A. L. Weber, F. J. Ramos, M. K. Nazeeruddin, M. Grätzel, D. Li, A. L. Domanski, I. Lieberwirth, S. Ahmad, and R. Berger, *Nat. Commun.*, 2014, **5:5001**, 1–9

11.H. Li, K. Fu, A. Hagfeldt, M. Gratzel, S. G. Mhaisalkar and A. C. Grimsdale, *Angew. Chem., Int. Ed.*, 2014, **53**, 4085-4088.

12.N. J. Jeon, J. Lee, J. H. Noh, M. K. Nazeeruddin, M. Gratzel and S. I. Seok, *J. Am. Chem. Soc.*, 2013, **135**, 19087-19090.

13.J. Wang, S. Wang, X. Li, L. Zhu, Q. Meng, Y. Xiao and D. Li, *Chem. Commun*., 2014, **50**, 5829-5832.

14 .S. Lv, L. Han, J. Xiao, L. Zhu, J. Shi, H. Wei, Y. Xu, J. Dong, X. Xu, D. Li, S. Wang, Y. Luo, Q. Meng and X. Li, *Chem. Commun*., 2014, **50**, 6931-6934.

15. N. J. Jeon, H. G. Lee, Y. C. Kim, J. Seo, J. H. Noh, J. Lee and S. I. Seok, *J. Am. Chem. Soc*., 2014, **136**, 7837-7840.

16. P. Qin, S. Peak, M. I. Dar, N. Pellet, J. Ko, M. Gratzel and M. K. Nazeeruddin, *J. Am. Chem. Soc*., 2014, **136**, 8516-8519.

17.J. A. Christians , R. C. M. Fung , P. V. Kamat , J. Am. Chem. Soc. 2014 , **136** , 758-764 .

18. A. S. Subbiah , A. Halder , S. Ghosh , N. Mahuli , G. Hodes , S. K. Sarkar , *J. Phys. Chem. Lett*. 2014 , **5** , 1748-1753 .

19. J. H. Heo, S. H. Im, J. H. Noh, T. N. Mandal, C.-S. Lim, J. A. Chang, Y. H. Lee, H. Kim, A. Sarkar, M. K. Nazeeruddin, M. Gratzel and S. Seok II, *Nat. Photonics*, 2013, **7**, 486–491.

20.J. H. Noh, S. H. Im, J. H. Heo, T. N. Mandal and S. I. Seok, *Nano Lett*., 2013, **13**, 1764–1769.

21. C. V. Kumar, G. Sfyri, D. Raptis, E. Stathatos and P. Lianos, *RSC Adv.*, 2015, **5**, 3786-3791.

22. F .Javier Ramos,M. Ince, M. Urbani, A.Abate, M. Gratzel, S.Ahmad, T.Torres, M. K. Nazeeruddin, *Dalton Trans.***,** 2015,**44**, 10847-10851

23. H. Xu, X.-J.Jiang, E. Y. M. Chan, W-P Fong, D. K. P. Ng, *Org. Biomol. Chem*.2007, **5**, 3987-3992.

24. C.G Claessens, D.Gonzalez-Rodriguez, T.Torres, *Chem. Rev.* 2002,**102**, 835-854.

25. D. D. Diaz, H. J. Bolink, L, Cappelli, C. G Claessens, E.Coronado, T.Torres, *Tetrahedron Lett*.2007, **48**, 4657-4660.

26.H. Gommans, D. Cheyns, T.; Aernouts, C. Birotto, J. Poortmans, P.Heremans, *.Adv. Funct.Mater*. 2007, **17**, 2653-2658.

27.L. Etgar, P. Gao, Z. Xue, Q. Peng, A. K. Chandiran, B. Liu, M. K. Nazeeruddin, and M. Grätzel, *J. Am. Chem. Soc.* 2012,**42**,17396–17399.

28. C. D. Zyskowski, V. O. Kennedy, *J. Porphyrins Phthalocyanines.* 2000, **4**, 707-712.

29. G.Sfyri, C.V.Kumar, D.Raptis, V.Dracopoulos, P.Lianos, *Sol.Energ.Mat.Sol.C.,*2015, **134**, 60–63

30.K.L. Mutolo, E.I. Mayo, B.P. Rand, S.R. Forrest, M.E. Thompson, *J. Am. Chem. Soc*. 2006,**128**,8108–8109.

31. M. Antoniadou, E. Siranidi, N. Vaenas, A. G. Kontos, E. Stathatos, and P. Falaras, *J. Surf. Interfac. Mater,* 2014,**2**,1-5.

32. G.Niu, W.Li, F.Meng, L.Wang, H.Dong, and Y.Qiu, *J.Mater.Chem. A,* 2014, **2**,705-710.

33. G.Niu, X.Guo and L.Wang, *J.Mater.Chem. A,* 2015, **3**, 8970-8980.

Table 1: *Current-Voltage* characteristics of photovoltaic measurements

HTM	Day[+]	V_{oc} (V)	J_{sc} (mA/cm^2)	FF (%)	η (%)
SubPc	**1**	**0.60**	**14.0**	**40**	**3.4**
-//-	2	0.61	15.1	40	3.7
-//-	3	0.61	16.7	40	4.1
-//-	4	0.62	16.9	41	4.3
-//-	5	0.63	18.9	41	4.9
-//-	6	0.64	19.1	42	5.4
-//-	7	0.64	20.2	44	5.7
-//-	8	0.67	20.5	46	6.3
-//-	**9**	**0.67**	**21.3**	**46**	**6.6**
-//-	10	0.66	20.1	40	5.3
-//-	11	0.66	19.6	39	5.0
-//-	12	0.67	18.4	37	4.6
CuPc	-	**0.67**	**19.2**	**40**	**5.0**

[+]Day since cell assembly, where day 1 is the day of cell assembly

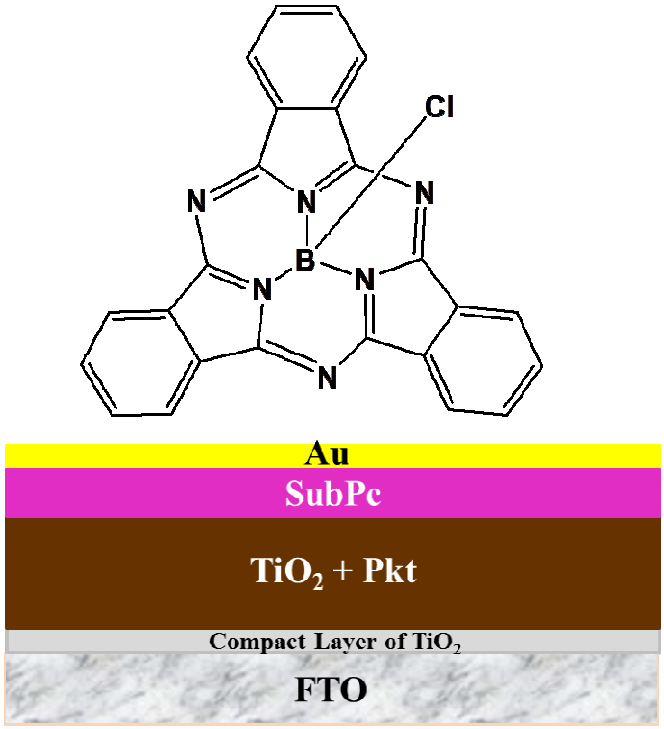

Figure 1. Molecular structure of subphthalocyanine (SubPc) and device architecture of the perovskite solar cell

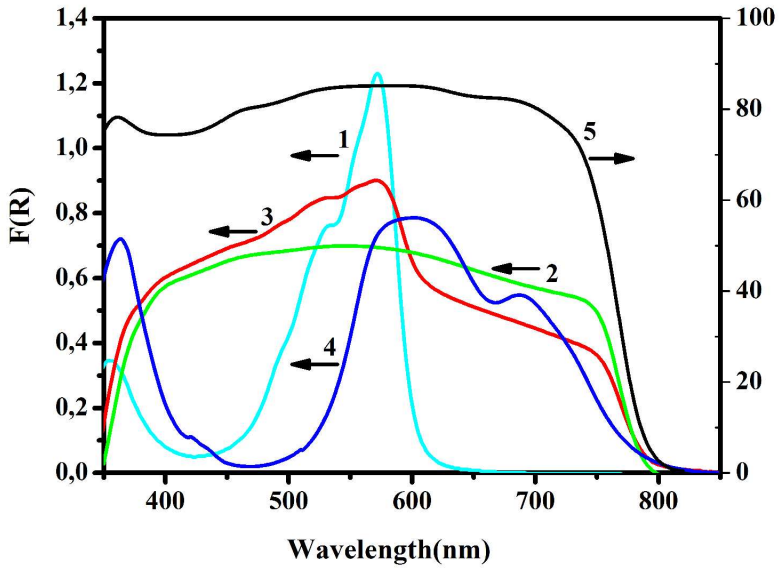

Figure 2. UV-vis absorption spectra of (1) SubPc on mesoporous TiO_2; (2) $CH_3NH_3PbCl_xI_{3-x}$ on mesoporous titania; (3) SubPc/$CH_3NH_3PbCl_xI_{3-x}$ /TiO_2; (4) Copper phthalocyanine on mesoporous TiO_2; and (5) IPCE% spectrum for the SubPc/$CH_3NH_3PbCl_xI_{3-x}$ /TiO_2 solar device.

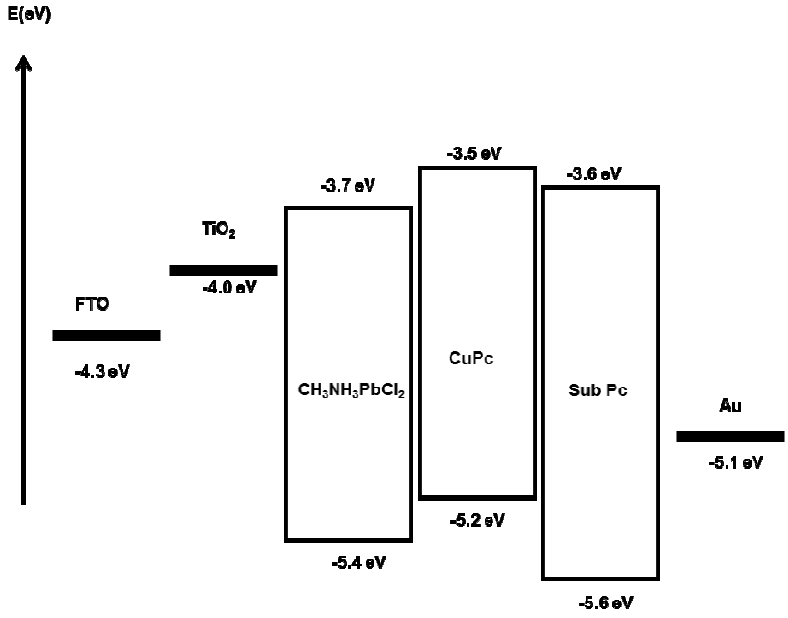

Figure 3. Energy level diagram of perovskite solar cells comprising subphthalocyanine[30] in comparison with copper phthalocyanine[21].

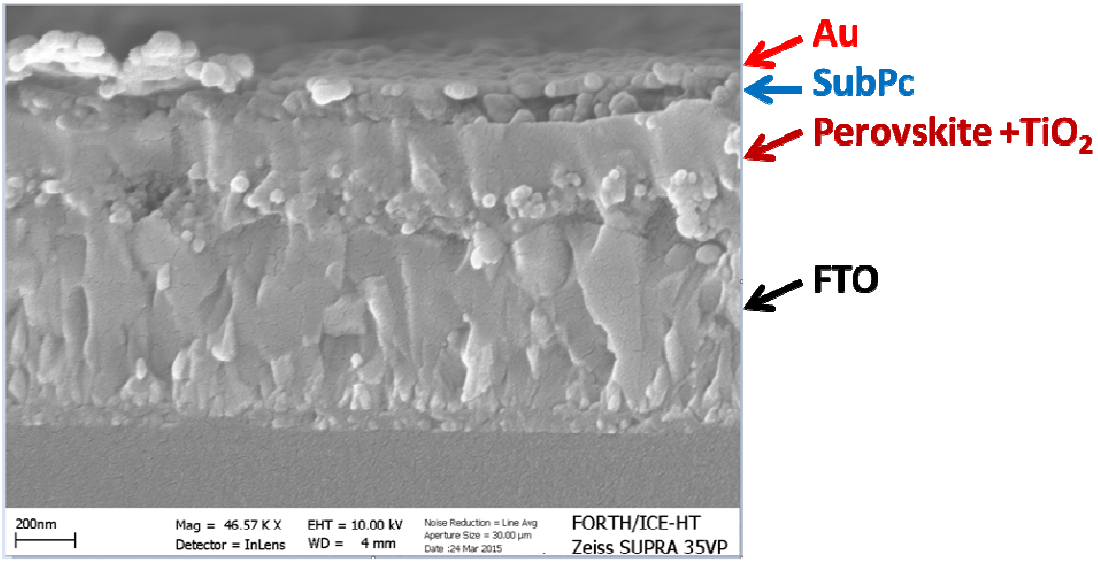

Figure 4. A cross-sectional image of FTO/ TiO_2/$CH_3NH_3PbCl_xI_{3-x}$ /SubPc/Au

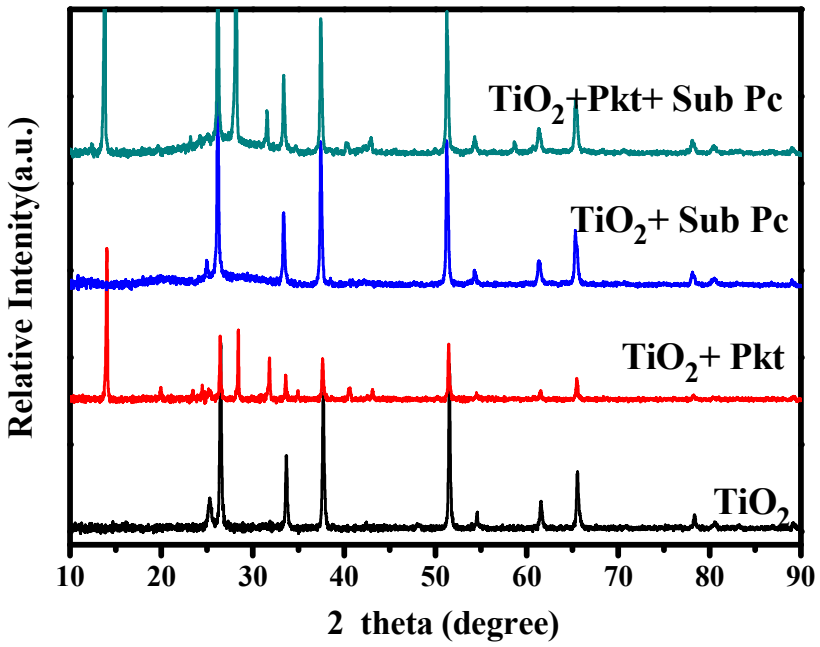

Figure 5. XRD diffractograms of various film combinations. The abbreviation Pkt stands for perovskite.

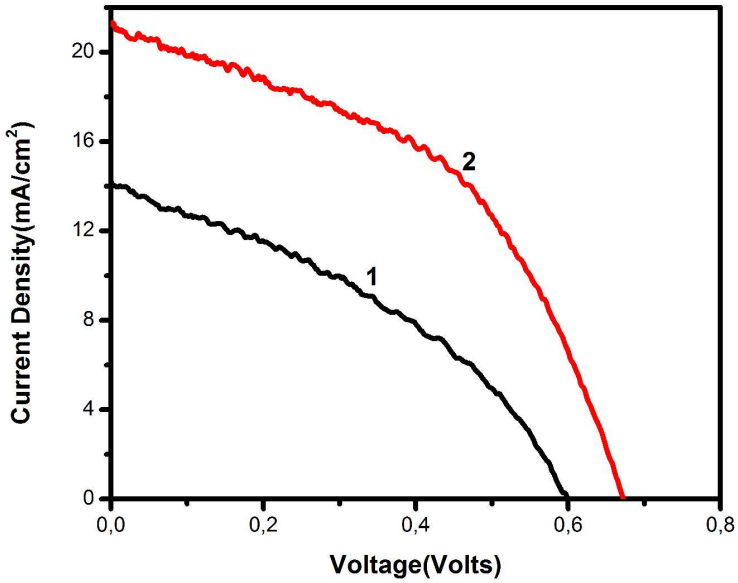

Figure 6. Current-voltage characteristics of the best FTO/TiO_2/ $CH_3NH_3PbCl_xI_{3-x}$/SubPc/Au cell: (1) 1st day and (2) 9th day

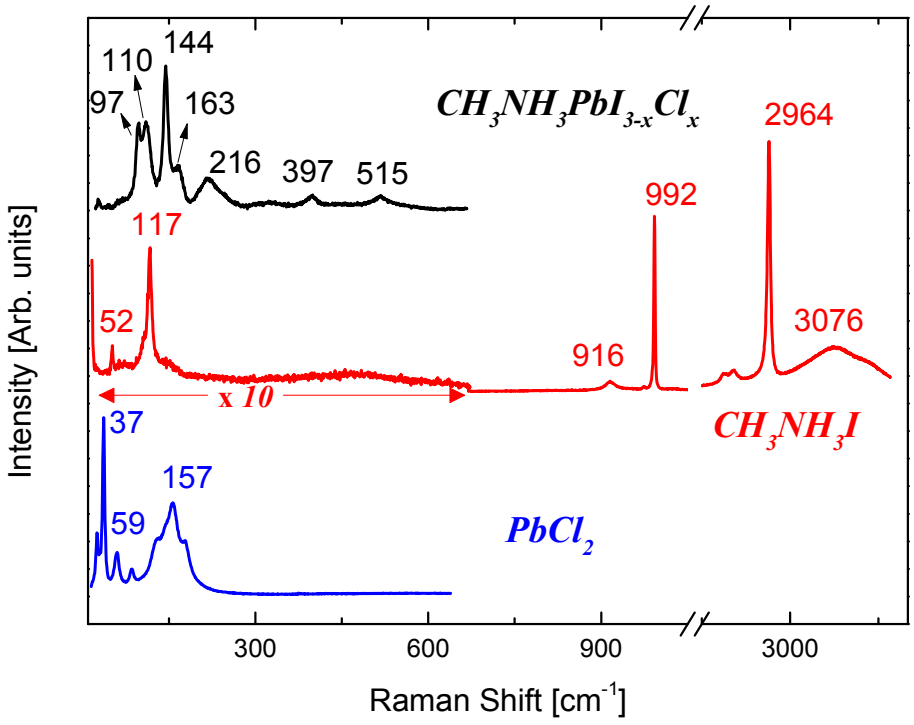

Figure 7. Raman spectra for the precursor samples ($PbCl_2$ and CH_3NH_3I) under inert atmosphere, as well as for the perovskite material $CH_3NH_3PbCl_xI_{3-x}$ under ambient conditions.

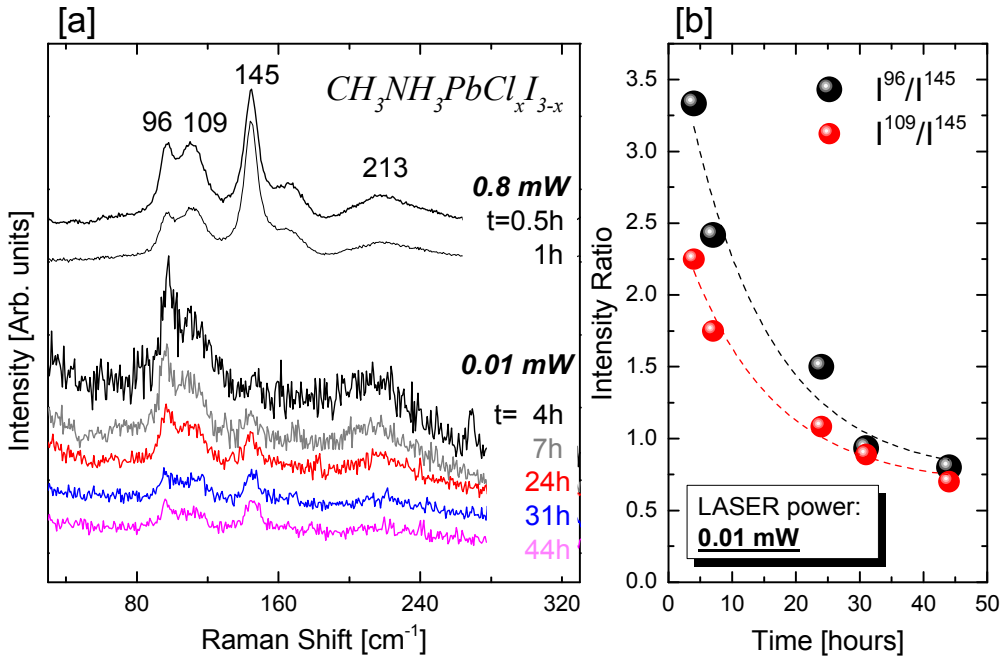

Figure 8. [a] Raman spectra of perovskite as a function of time using 0.8 mW and 0.01 mW laser power on sample. [b] Intensity ratio of two of the perovskite bands (96 cm^{-1} and 109 cm^{-1}) with respect to the anatase band at 145 cm^{-1}, as a function of time for the case of low laser power (0.01 mW).